

*Research article*

## Comprehensive assessment of air pollutant and noise emissions at airports across different altitudes

Weizhen Tang, Jie Dai\* and Zhousheng Huang

College of Air Traffic Management, Civil Aviation Flight University of China, Guanghan, 618300, China

\* **Correspondence:** Email: [daij8824@gmail.com](mailto:daij8824@gmail.com).

**Abstract:** We utilized the International Civil Aviation Organization (ICAO) standard emission model, refined with adjustments for fuel flow, LTO cycle work mode time, and emission indices, to investigate the environmental footprint of airports at different altitudes. Airports categorized as high (above 5000 ft), medium (1500–5000 ft), and low (below 1500 ft) altitudes were selected to provide a comprehensive representation of the altitude spectrum. The analysis was anchored over the period spanning 2016 to 2017. Emission inventories for air pollutants and noise were computed for these airports, focusing on the LTO (Landing and Take-Off) cycle. Our findings indicated that high altitude airports exhibit the highest  $\text{NO}_x$  emissions, reaching 406.4 t, whereas low altitude airports record the highest noise levels at 73.1 dB. Significant disparities in emission profiles were observed across different phases of the LTO cycle at airports of varying altitudes. Notably, during the climb phase, the types and proportion of  $\text{NO}_x$  emissions at high altitude airports were as high as 71.8%, contrasting with the 45.6% at low altitude airports. Additionally, emissions of gaseous pollutants from major aircrafts, exemplified by the A320 model, escalated with altitude. Specifically,  $\text{NO}_x$  emissions increased from 10.55 kg/cycle at low altitude to 20.48 kg/cycle at high altitude, and CO emissions from 10.88 kg/cycle to 22.89 kg/cycle. A robust correlation between  $\text{NO}_x$  emissions and  $L_{den}$  was identified among airports at different altitudes, with correlation coefficients of 0.96 for low altitude, 0.97 for medium altitude, and 0.93 for high altitude airports. This study delineates the distinct characteristics of air pollutant and noise emissions from airports across altitudes, offering novel insights for the environmental assessment of airport operations.

**Keywords:** different altitudes; air pollutants; noise emissions; emission inventories; corrective modeling assessment; LTO cycle

---

## 1. Introduction

Against the background of the rapid development of the global aviation industry, the issue of aircraft emissions is a growing concern. Air pollutants such as nitrogen oxides ( $\text{NO}_x$ ), carbon monoxide (CO), hydrocarbons (HC) and sulfur dioxide ( $\text{SO}_2$ ) generated by aircraft during take-off and landing, taxiing, and climbing phases have significant impacts on air quality and health of residents in the vicinity of airports [1–4]. In addition, noise pollution from aircraft landings and takeoffs causes damage to the environment and poses a serious threat to human health [5–7]. Most studies show that aircraft emissions are an important source of pollution that seriously affects air quality in the vicinity of airports and poses a negative threat to people's health, livelihood and comfort [8–10].

Researchers looking at domestic and international areas on airport emissions mainly focus on low and medium altitude airports in large cities, and they consider only the impact of air pollutant emissions on the environment and not the impact of noise pollution on the areas adjacent to the airport. In the urban scale study, Wasiuk DK et al. [11] conducted a comprehensive analysis of the atmospheric emission inventory for airports at mid and low altitudes globally, utilizing the Boeing Fuel Flow Method 2 (BFFM2) for calculating aircraft emissions. The results demonstrated a significant enhancement in the precision of the model's calculations. Many scholars in China have measured pollutant emissions from individual airports at low altitude, such as Beijing Capital International Airport [12–15], Beijing Daxing International Airport [16], Shanghai Pudong International Airport [17], and Guangzhou Baiyun International Airport [18] and assessed the impacts on air quality around the airports. In regional scale studies, Chinese researchers have carried out emission inventory calculations for airport clusters such as the Yangtze River Delta [17,19] and Beijing-Tianjin-Hebei [16,20] and analyzed the spatial distribution of pollutants on a regional scale. In the study of aircraft noise, Du et al.[21] predicted and prevented aircraft noise pollution in Tianjin airport based on the INM model; Cheng et al.[22] proposed countermeasures to prevent and control aircraft noise by describing the impacts of aircraft noise and aircraft acoustic explosions; and Mato RR et al.[23] evaluated the noise pollution related to airport operation based on Dar Es Salaam International Airport and analyzed the takeoffs of aircraft, landing is the main source of noise pollution.

However, compared with the research on pollutant emissions at the urban scale and the horizontal regional scale, China's research on the emission characteristics of the vertical region is relatively weak, and many studies analyze only the emission inventory without considering the environmental impact of the noise generated by aircraft takeoff and landing. Based on this, we adopt the ICAO advanced method as the basis for correcting the emission parameters and more accurately calculate the annual air pollutant emission inventories of three different altitude airports in the 2016–2017 flight season, while introducing the index of noise for the first time, adopt A-weighting to correct it to be more in line with the real sound level, aiming to explore the emission characteristics of airports of different altitudes and their noise impact on the environment, and provide an opportunity for improving the environmental management of airports at different altitudes and the environmental management of airports in different regions. Our purpose is to explore the emission characteristics of airports at different altitudes and their noise impact on the environment, so as to provide a scientific basis for improving the environmental management and assessment of airports at different altitudes.

## 2. Materials and methods

### 2.1. Subjects of study

The area of this study covers medium-sized civil aviation airports with a comparable number of LTO cycles/year at three different altitudes. ICAO standards for high altitude airports: High altitude airports are airports with altitudes of 5000 ft and above [24]. Since the document does not specify the specific altitude of low and medium altitude airports, we select 5000 ft as high-altitude airports, 1500–5000 ft as medium altitude airports, and below 1500 ft as low altitude airports. Taking October 2016 to September 2017 as the base period, a certain three different altitude types of airports in China are selected, which are a high-altitude airport (altitude 11719.2 ft), a medium-altitude airport (altitude 1624.2 ft), and a low-elevation airport (altitude 16.4 ft). These airports represent a wide range of airports, from low altitude to high altitude airports. The study was conducted on incoming and outgoing civil aircraft at these regional airports, and the emission inventories covered gaseous pollutants ( $\text{NO}_x$ , HC, CO,  $\text{SO}_2$ ) and day-evening-night average noise level ( $L_{den}$ ).

### 2.2. Data sources

According to ICAO, aircraft activities at airports can be described by the LTO cycle, which includes four operating modes: Approach, taxi, takeoff, and climb, and we follow the LTO cycle classification method to carry out the air pollutant emission inventory calculation. It has been shown that the factors affecting air pollutant emissions from aircraft include: Aircraft type, aircraft model, and its corresponding engine, operating mode, emission factor per unit of fuel consumption rate under each mode, and operating time [25]. For this reason, we summarize the investigation of civil aviation aircraft landing and taking off at three different altitude airports, as follows.

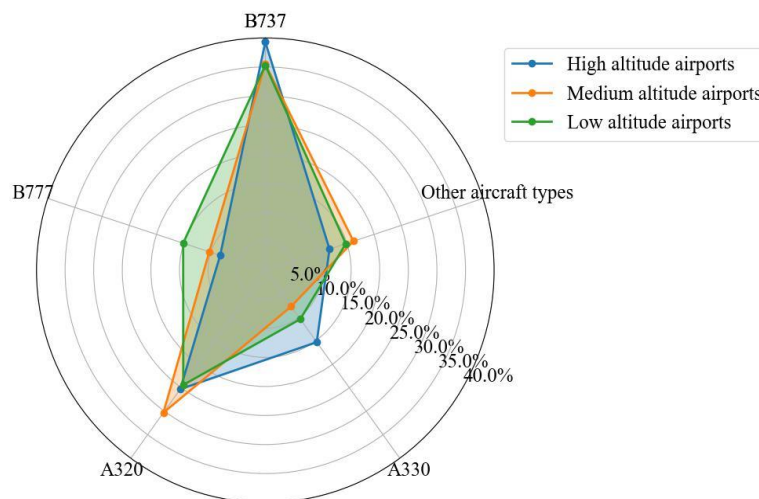


**Figure 1.** Proportion of aircraft types at airports of different altitudes.

① Aircraft type (All aircraft are assumed to always be at maximum takeoff weight (MTOW)): According to the flight information published online by a total of 29 domestic and foreign airlines, the main types of civil aircraft at three different altitude airports include four major categories, namely

B737, B777, A320 and A330, which account for the percentage shown in Figure 1. As can be seen, civil passenger aircraft at high altitude airports accounted for 39.3%, 8.3%, 25.3%, and 11.8%. Civil passenger aircraft at medium altitude airports accounted for 35.5%, 10.3%, 30.3%, and 7.7%. Civil passenger aircraft at low altitude airports accounted for 35.3%, 15.1%, 24.4%, and 10.4%.

②Determination of operating modes: The rated thrust and operating time of the aircraft in each mode of the LTO cycle mainly refer to the recommended parameters of ICAO, in which the rated thrust of the four operating modes of taxiing, approach, climb, and takeoff are set to 7%, 30%, 85%, and 100%, and the operating time is 26, 0.4, 2.2, and 0.7 min, as shown in Figure 2. The ICAO regulations for the climb mode mainly refer to the end of the takeoff to the end of the aircraft rushed to the top of the atmospheric boundary layer at an altitude of about 3000 ft [26].

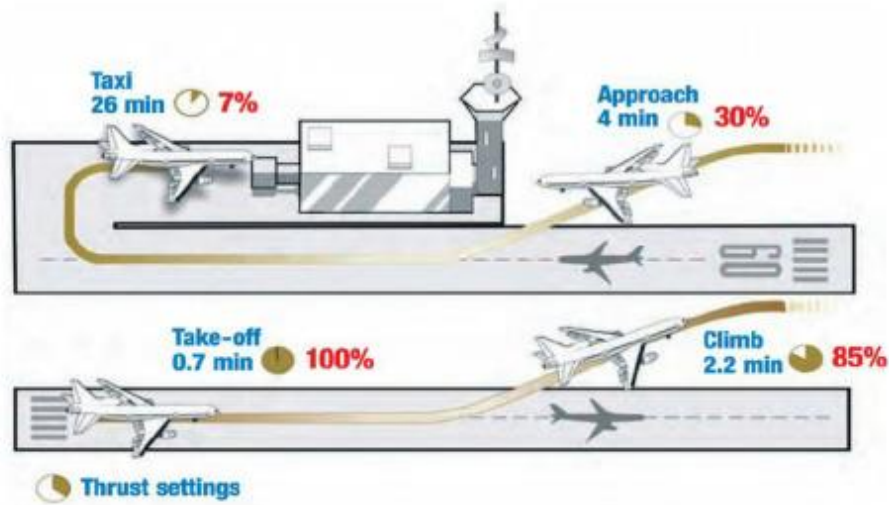


**Figure 2.** ICAO Manual Emissions Certification LTO Cycle.

③Fuel consumption rate and emission factor in each operating mode: The fuel consumption rate of the engine in each operating mode and the emission factors of  $\text{NO}_x$ , HC, and CO are taken from ICAO Aircraft Engine Emission Database [26].

### 2.3. Calculation models for gaseous pollutants

ICAO three methods are given for calculating aircraft engine emissions: The simple method, the advanced method, and the complex method. Considering the accuracy, generality, feasibility, and economy of the calculation methods, the calculation is based on the advanced method of ICAO, and the basic formula is

$$E_{w,j,m} = \sum t_{w,m} \times FF_{w,m} \times EI_{w,j,m} \times n_w \quad (1)$$

where  $E_{w,j,m}$  is the emissions of the pollutant  $j$  for the model  $w$  during the flight phase  $m$ , g;  $t_{w,m}$  is the flight time of the model  $w$  during the flight phase  $m$ , min;  $FF_{w,m}$  is the fuel consumption of the model  $w$  during the flight phase  $m$ , kg/s;  $EI_{w,j,m}$  is the index of the emissions of the pollutant  $j$  for the model  $w$  during the flight phase  $m$ , g/kg;  $n_w$  is the number of engines installed.

The BFFM2 method [27] was used to further optimize the fuel flow rate, flight time and emission index in equation (1).

### 2.3.1. Fuel flow correction

The fuel flow rates in the standard ICAO database are values at standard sea level altitude and standard atmospheric conditions. The actual fuel flow rate needs to be converted to values at standard sea level and standard atmospheric conditions before segmental linear interpolation is performed. The conversion formula is

$$FF_i = FF_0 \frac{\lambda^{3.8}}{\mu} e^{0.2Ma^2} \quad (2)$$

In the formula,  $FF_i$  is the corrected fuel flow rate of a single engine, kg/s;  $FF_0$  is the actual fuel flow rate of a single engine, kg/s;  $\lambda$  is the ratio of outside temperature to the sea level temperature under standard atmospheric conditions;  $\mu$  is the ratio of outside air pressure to the sea level pressure under standard atmospheric conditions;  $T$  is the outside temperature,  $P$  is the outside air pressure; and  $Ma$  is the flight Mach number.

Barometric pressure is derived from flight altitude and outside temperature using a methodology provided by the Federal Aviation Administration (FAA). The calculation formula is as follows:

$$P = \begin{cases} P_0 \mu^{5.2579}, & H \leq H_{trop} \\ P_{trop} \exp \left[ -\frac{g}{RT_{trop}} (H - H_{trop}) \right], & H > H_{trop} \end{cases} \quad (3)$$

where  $P$  is the derived outside air pressure, Pa;  $P_0$  is the sea level pressure at standard atmospheric conditions, 1013.25 hPa;  $P_{trop}$  is the air pressure at the top of the troposphere, 226.19 hPa;  $g$  is the gravitational constant,  $9.81 \text{ m} \cdot \text{s}^{-2}$ ;  $R$  is the gas constant of the air,  $286.9 \text{ J} \cdot (\text{kg} \cdot \text{k})^{-1}$ ;  $T_{trop}$  is the temperature at the top of the troposphere, 216.65 K;  $H$  is the altitude of the flight, m; and  $H_{trop}$  is the altitude at the top of the troposphere, 11000 m.

### 2.3.2. LTO time correction

The ICAO specifies the climb pattern of an airplane, which mainly refers to the altitude from the end of takeoff to the ascent to the mixed layer of the atmosphere (fixed at 3000 ft), but the height of the mixed layer in actual operation changes with time, place, and meteorological conditions, and the calculation of the altitude using 3000 ft specified by ICAO will produce a large error. In this study, the EPA method is used to correct the climb and approach reference time specified by ICAO, and the correction formula is as follows.

$$T_C = t_C \times \frac{H_M - 553.04}{2446.96} \quad (4)$$

$$T_A = t_A \times \left( \frac{H_M}{3000} \right) \quad (5)$$

In the formula,  $T_C$  and  $T_A$  denote the actual operating time of the approach and climb phases of the aircraft (min);  $t_C$  and  $t_A$  denote the reference time of the approach and climb of the ICAO specified aircraft, which are 4.0 and 2.2 min, respectively.  $H_M$  denotes the actual maximum mixed layer height of an airport.

### 2.3.3. Emission index corrections

Taking the flight altitude and outside temperature provided by the logger data, the emission index is corrected for the environment, and the correction formula is

$$EI_j = \begin{cases} \frac{EI_0 \theta^{3.3}}{\delta^{1.02}}, j = HC \text{ or } CO \\ EI_0 \left( \frac{\delta^{1.02}}{\theta^{3.3}} \right)^{0.5} e^S, j = NO_x \end{cases} \quad (6)$$

$$S = 19.0 \left( 0.0063 - \frac{0.622 \varphi P_v}{P - \varphi P_v} \right) \quad (7)$$

where  $EI_j$  is the corrected emission index of the exhaust gas  $j$ , g/kg;  $S$  is the humidity factor;  $\varphi$  is the relative humidity of the atmosphere.  $P_v$  is the saturated vapor pressure, Pa. Where  $EI_0$  is the preliminary corrected exhaust emission index, g/kg. In this study, we refer to Huang M et al. [28] who used segmented linear interpolation to correct the emission index. The FAA fits the logarithm of the HC and CO emission indices as a piecewise linear function of the logarithm of the fuel flow, and the logarithm of the emission index of  $NO_x$  is fitted as a linear function of the logarithm of the fuel flow rate, so as to characterize the variation of the exhaust emission index with the fuel flow rate. Therefore, based on the converted fuel flow rate, the segmented linear interpolation of the emission index was calculated by the equation

$$EI_0 = \begin{cases} \frac{(EI_{TO} - EI_C)(FF_M - FF_C)}{FF_{TO} - FF_C}, FF_M \geq FF_C \\ \frac{(EI_C - EI_A)(FF_M - FF_A)}{FF_C - FF_A}, FF_A \leq FF_M \leq FF_C \\ \frac{(EI_A - EI_I)(FF_M - FF_I)}{FF_A - FF_I}, FF_M < FF_A \end{cases} \quad (8)$$

where  $EI_{TO}$ ,  $EI_C$ ,  $EI_A$ , and  $EI_I$  are the standard emission indices for the takeoff, climb, approach and taxi phases given by the ICAO database, g/kg;  $FF_{TO}$ ,  $FF_C$ ,  $FF_A$ ,  $FF_I$  are the standard fuel flow rates for individual engines for the takeoff, climb, approach and taxi phases given by the ICAO database, g/kg.

Since ICAO does not provide a standard methodology for calculating emissions from  $SO_2$ , it is set to 1 g/kg [29].

## 2.4. Airport noise calculation model

There are no internationally harmonized standards. In general, noise metrics can be categorized into three types: Single event noise metrics, cumulative exposure metrics and daily metrics. In this paper, cumulative exposure metrics are chosen, which are used to quantify the noise impact caused by multiple aircraft movements within a given time frame.

### 2.4.1. A-weighted sound pressure level ( $L_A$ ) formulae

The human ear is sensitive to sound frequencies between 20 Hz and 20000 Hz, especially around 4000. A-weighting weakens the low and high frequency measurements and emphasizes the mid-

frequency measurements. The adjusted result better reflects the actual sound heard by the human ear. The formula is

$$L_A = 20 \cdot \log_{10} \left( \frac{P}{P_0} \right) - 20 \cdot \log_{10} \left( \frac{f}{1000} \right) \quad (9)$$

where  $L_A$  is the A-weighted sound pressure level in decibels;  $P$  is the measured sound pressure;  $P_0$  is the reference sound pressure, usually taken as 20  $\mu$ Pa, which corresponds to the smallest sound pressure that can be heard by the human ear; and  $f$  is the frequency of the sound in hertz.

#### 2.4.2. A-weighted equivalent continuous sound level ( $L_{Aeq,T}$ ) calculation formula

The  $L_{eqT}$  metric measures the average sound pressure level over a certain time interval and can be used to evaluate the cumulative effect of all noise events occurring during a reference time interval. Similarly,  $L_{Aeq,T}$  is the equivalent continuous sound level weighted by A. The  $L_{eqT}$  metric is a good reflection of the social nuisance caused by aircraft noise, and it has become the most widely used noise metric internationally. It has become the most widely used noise metric internationally. The US EPA uses it as the basic descriptive metric for noise measurements. According to the ISO 20906 standard [30], the  $L_{Aeq,T}$  metric is calculated as follows:

$$L_{Aeq,T} = 10 \log_{10} \frac{\frac{1}{T} \int_{t_1}^{t_2} P_A^2(t) dt}{P_0^2} \quad (10)$$

where  $P_A(t)$  is the A weighted instantaneous sound pressure for the runtime ( $t_1 - t_2$ );  $P_0$  is the reference air pressure, usually taking the value of 20  $\mu$ Pa;  $T$  is the time experienced by  $t_1 - t_2$ .

#### 2.4.3. Day-evening-night average noise level ( $L_{den}$ ) calculation formula

The  $L_{den}$  gauge is a combined gauge based on the Equivalent Continuous Sound Level (ECSL) of  $L_{Aeq,T}$ , combining the  $L_{day}$  metric, the  $L_{evening}$  metric, the  $L_{night}$  metric, and adding 5 dB(A) and 10 dB(A) as penalty parameters to the values of  $L_{evening}$  and  $L_{night}$ , respectively. According to the instruction 2002/49/CE [31] and the advisory notice 150/5020-1 [32], the formula is calculated as follows:

$$L_{den} = 10 \log_{10} \left[ \frac{1}{24} \left( 12 \cdot 10^{\frac{L_{day}}{10}} + 4 \cdot 10^{\frac{L_{evening}+5}{10}} + 8 \cdot 10^{\frac{L_{night}+10}{10}} \right) \right] \quad (11)$$

where  $L_{day}$ ,  $L_{evening}$  and  $L_{night}$  are the weighted long-term average sound levels of A during the daytime(7:00 – 19:00), evening(19:00 – 23:00) and nighttime(23:00 – 7:00) for a year. The formulas for  $L_{day}$ ,  $L_{evening}$ , and  $L_{night}$  are as follows:

$$L_{day} = 10 \log_{10} \left( \frac{1}{12} \sum_{H=7}^{18} 10^{\frac{L_{Aeq,H}}{10}} \right) \quad (12)$$

$$L_{evening} = 10 \log_{10} \left( \frac{1}{4} \sum_{H=19}^{22} 10^{\frac{L_{Aeq,H}}{10}} \right) \quad (13)$$

$$L_{night} = 10 \log_{10} \left( \frac{1}{8} \sum_{H=23}^6 10^{\frac{L_{Aeq,H}}{10}} \right) \quad (14)$$

where  $H$  is the index of the hour of the day, e.g., when  $H = 4$  represents the hour from 4:00 to 4:59:59. The  $L_{Aeq,H}$  is  $L_{Aeq,T}$  for the hour  $H$ .

### 3. Results and discussion

#### 3.1. Emissions inventory results

The 2016–2017 LTO cycle emission inventory for airports at different altitudes is shown in Table 1, and based on equations 1 to 4, the total annual emissions of pollutants from aircraft takeoffs and landings at airports at different altitudes as well as the average daytime and nighttime noise levels are calculated as shown in Table 1. As can be seen in Table 1, the low altitude airports have 12,893 LTO /cycles and the lowest  $\text{NO}_x$  emissions of 254.0 t, whereas the average daytime and nighttime noise levels are the highest at 73.1 dB. In comparison, the medium altitude airport has 14,242 LTO /cycles and 263.3 t of  $\text{NO}_x$  emissions, and the average daytime noise level rises to 70.0 dB. High altitude airports have 13,734 cycles of LTO and emit a total of 406.4 t of  $\text{NO}_x$ , 26.4 t of HC, 242.2 t of CO, 20.4 t of  $\text{SO}_2$ , and an average daytime noise level of 61.9 dB.

**Table 1.** Inventory of Aircraft LTO Cycle Emissions at Airports of Different Altitudes, 2016–2017.

Elevation type	Type of airport	LTO cycles /times	Air pollutant emissions /t				$L_{den}$ /dB
			$\text{NO}_x$	HC	CO	$\text{SO}_2$	
Low altitude	Low altitude airports	12893	254.0	11.8	136.0	17.8	73.1
Middle altitude	Medium altitude airports	14242	263.3	9.3	143.2	24.5	70.0
High altitude	High altitude airports	13734	406.4	26.4	242.2	20.4	61.9

The difference between high, medium and low altitude airports in terms of LTO cyclic emissions can be visualized quite well in Figure 3. From the figure 3, it can be observed that the high-altitude airports are in the leading position in terms of  $\text{NO}_x$  emissions with significantly higher values than the medium and low altitude airports. The HC emissions of the airports are relatively average among the three and the difference is not significant. The CO emissions are similar to those of  $\text{NO}_x$ , with high altitude airports emitting the most. However, for  $\text{SO}_2$  emissions, the mid-elevation airports exhibit slightly higher emissions. The comparison of noise levels shows the highest value of 73.1 dB for low altitude airports, implying that noise pollution is more of a problem here. The comparison shows that there is a significant difference in the emissions and noise levels of airports at different altitudes. The high-altitude airports have the highest  $\text{NO}_x$  emissions while the low altitude airports show the worst performance in terms of noise level.



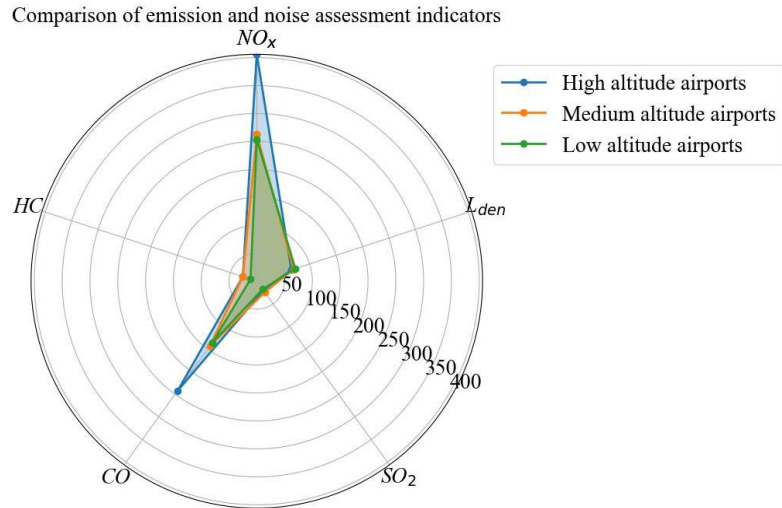


**Figure 3.** Comparison of emission and noise assessment indicators.

3.2. Emission sharing rates by mode of operation for airports at different altitudes

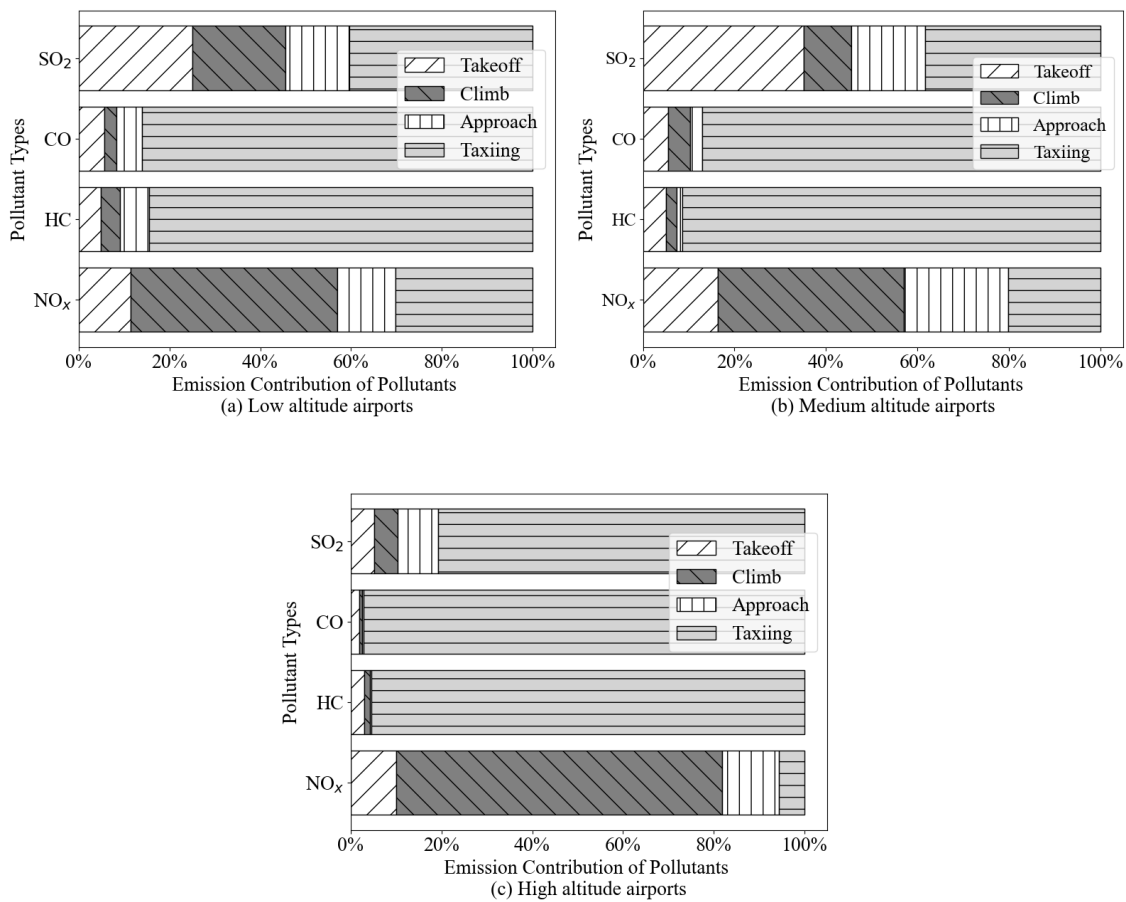


**Figure 4.** Air pollutant partitioning rates for various operating modes: (a) Low, (b) Medium, (c) High.

The analysis of the emission share of air pollutants in the operating modes of airports at different altitudes in Figure 4 shows that the emission characteristics of pollutants are significantly affected by altitude. At low altitude airports, the emission share of  $\text{NO}_x$  in the climb phase reaches 45.6%, which may be due to the fact that the airplane needs maximum thrust in this phase, resulting in higher engine combustion temperatures, which promotes the generation of  $\text{NO}_x$ . At the same altitude, HC and CO accounted for 84.4% and 86.1%, respectively, in the taxiing phase, which reflects the incomplete combustion problem of the engine during a low load operation. The high percentage of  $\text{SO}_2$  emissions in the coasting phase (40.3%) may be related to the high sulfur content of the fuel used at low altitude.

The emission share of  $\text{NO}_x$  decreases slightly to 40.7% during the climb phase at mid-altitude airports, probably due to the relatively low combustion temperatures resulting from the relatively thin air, which reduces the emissions from  $\text{NO}_x$ . The high proportion of HC and CO emissions (91.4% and 87.1% respectively) remain significant in the taxi phase, suggesting that the low load combustion efficiency during taxi remains a major influence even with altitude changes. The distribution of  $\text{SO}_2$  shows that the take-off and taxiing stages are relatively average, accounting for 38.3% and 35.1% respectively, which may be related to the improvement of combustion conditions in mid-altitude airports.

Emissions at high altitude airports are particularly well characterized, with  $\text{NO}_x$  spiking to 71.8% in the climb phase, which is speculated to be likely due to the extra fuel input required by the engine to maintain thrust in thin air conditions, which results in a high percentage of  $\text{NO}_x$  emissions. While HC and CO contribute the most in the taxiing phase, 95.4% and 97.1% respectively, which implies that at high altitude, incomplete combustion is exacerbated by thin air even at low power conditions. The high share of  $\text{SO}_2$  emissions in the coasting phase 80.7% may be attributed to incomplete sulfur combustion conversion due to insufficient fuel combustion at high altitude conditions [33].

### 3.3. Comparison of single-day emissions and average diurnal noise levels at airports of different altitudes

The concentrations of  $\text{NO}_x$ , HC, CO,  $\text{SO}_2$  and  $L_{den}$  at airports of different altitudes during the period from October 2016 to September 2017 were calculated by correcting the computational model. As shown in Figure 5, the median and interquartile spacing of each pollutant showed a decreasing trend with increasing altitude, and the decrease in the concentrations of  $\text{NO}_x$  and HC was particularly obvious. Most of the daily emissions from  $\text{NO}_x$ , HC, CO, and  $\text{SO}_2$  at the lower elevation airports are centered around 710 kg, 35 kg, 370 kg, and 42 kg, respectively, while the average diurnal noise level is around 71 dB. This phenomenon may be related to the relatively increased air density in the region, resulting in inhibited diffusion and dilution of pollutants in the atmosphere, especially within the boundary layer near the ground. The greater air density may also increase the efficiency of sound wave propagation and enhance sound perception.

Pollutant concentrations and average daytime and nighttime noise levels at mid-altitude airports are moderate, with emissions at  $\text{NO}_x$ , HC, CO, and  $\text{SO}_2$  similar to those at low-altitude airports, centered around 750 kg, 38 kg, 380 kg, and 43 kg, respectively, and with noise levels around 80 dB. This suggests that pollutant and noise propagation begin to be influenced by atmospheric conditions at this altitude range. These airports may be in a transition zone where the atmospheric conditions are neither as thick nor as thin as at lower altitudes, so that the distribution of pollutants and noise is relatively equalized in these areas.

For high altitude airports, significant increases in daily emissions were observed at  $\text{NO}_x$ , HC, CO, and  $\text{SO}_2$ , concentrated around 1150 kg, 79 kg, 680 kg, and 48 kg, respectively, while the average diurnal noise level decreased to about 62 dB. The reduction in noise levels at high-altitude airports

can be attributed to the rarefied atmospheric conditions, which result in lower thrust production by aircraft engines, consequently leading to relatively lower noise levels. Furthermore, these conditions facilitate the rapid dispersion of gases and diminish the propagation efficiency of sound waves, contributing to lower ambient noise levels. The increased emissions at high-altitude airports may be due to two primary factors. First, in regions of high altitude, the scarcity of air compels aircraft engines to operate under varied conditions. Although the engines' relatively lower thrust at high altitudes may lead to reduced noise levels, the combustion efficiency of the engines may be compromised, thereby increasing the emissions of unburned hydrocarbons and nitrogen oxides. This phenomenon arises from the reduced oxygen concentration in the air, which hinders complete fuel combustion and subsequently augments the emission of pollutants [34–36]. Second, meteorological conditions in high-altitude areas are typically more complex, with lower temperatures and higher humidity levels potentially impacting the dispersion and deposition of pollutants. Meteorological factors, such as temperature inversion layers, can lead to the accumulation of pollutants in localized areas, making them less likely to disperse and resulting in higher measured concentrations of pollutants.

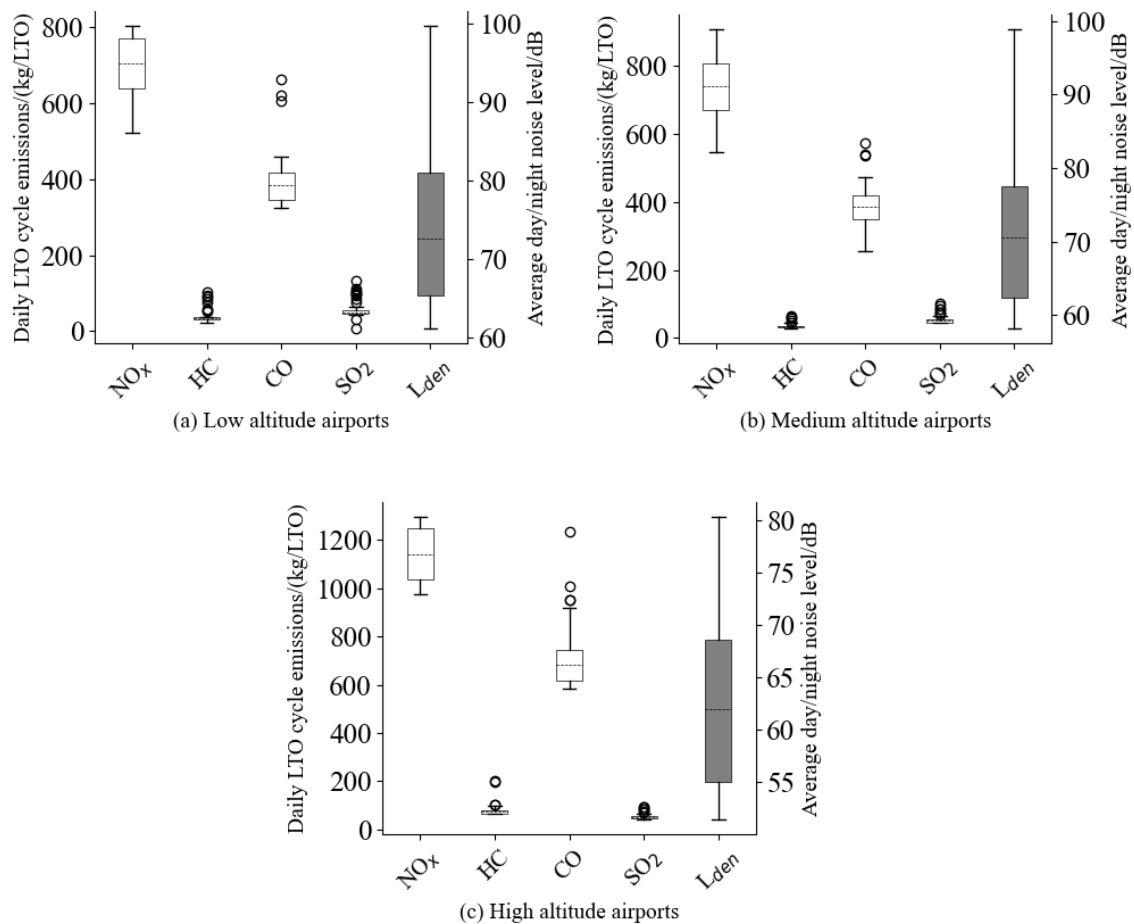


**Figure 5.** Single-day LTO cyclic emissions from airports: (a) Low, (b) Medium, (c) High.

### 3.4. Correlation between emissions and noise

The correlation coefficients of emissions from airports at different altitudes are shown in Figure 6. At low altitude airports, the correlation coefficient between NO<sub>x</sub> and  $L_{den}$  is 0.96, showing a very

strong positive correlation. This high correlation indicates that the increase in the emission of  $\text{NO}_x$ , one of the major aircraft emissions is accompanied by a significant increase in  $L_{den}$ . This high correlation may be highly correlated with the density of air traffic and frequency of flights, and it is further hypothesized that high temperatures at low altitudes may exacerbate the production rate of  $\text{NO}_x$ . In contrast, the correlation coefficient between HC and CO is 0.45, which is weaker than that between  $\text{NO}_x$  and  $L_{den}$ , but indicates a certain degree of positive correlation. This may be due to increased emissions from incomplete combustion of the fuel, which also leads to increased concentrations of HC and CO.

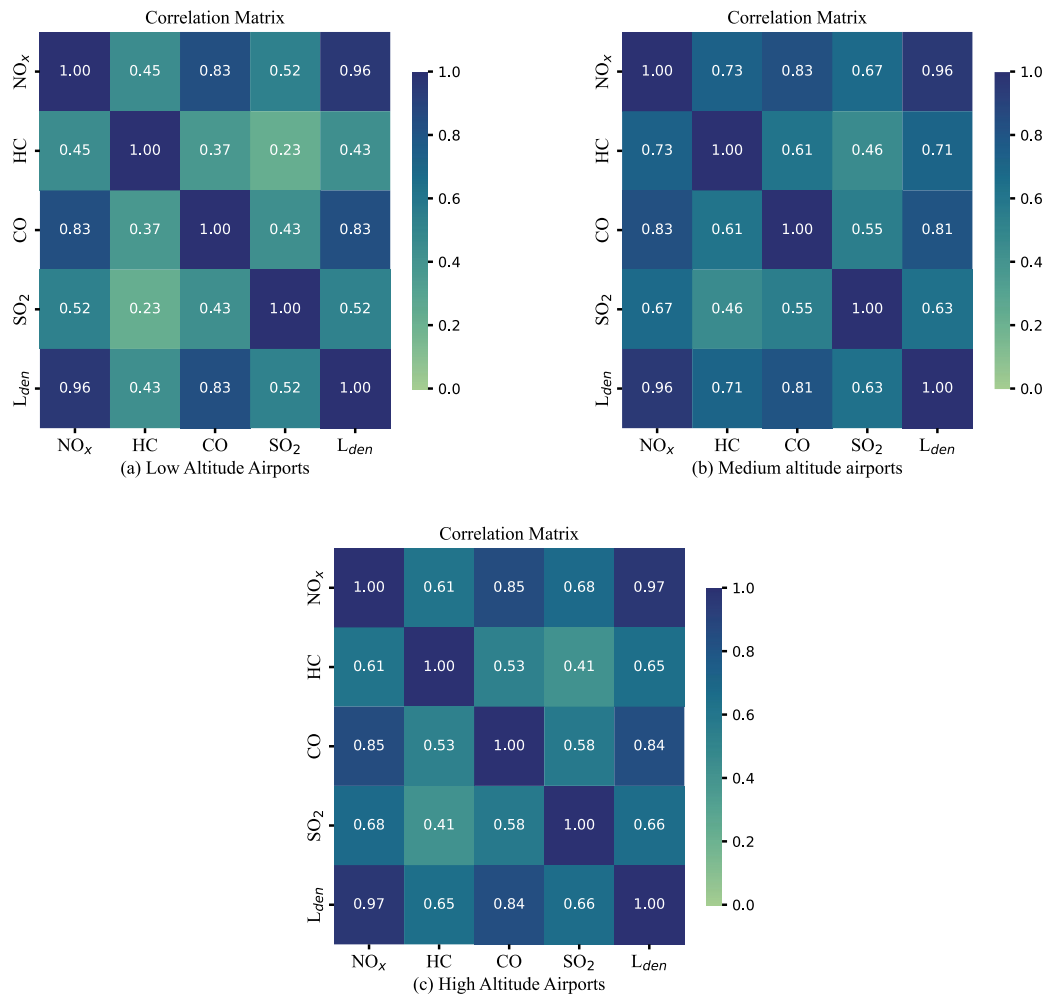


**Figure 6.** Matrix of correlation coefficients for emissions from airports: (a) Low, (b) Medium, (c) High.

This finding is further strengthened by the data from mid-altitude airports, where the correlation coefficient between  $\text{NO}_x$  and  $L_{den}$  is 0.97, showing a stronger positive correlation, which may be related to the changes in the combustion efficiency of the engine and the changes in the noise propagation characteristics due to the increase in altitude. In addition, the correlation coefficient between HC and CO increases to 0.61 at this altitude, indicating that the effect of incomplete combustion is more significant at mid-altitude airports compared to lower altitudes.

At high altitude airports, although the correlation coefficient between  $\text{NO}_x$  and  $L_{den}$  has decreased to 0.93, suggesting that other environmental factors such as climatic conditions and aircraft tuning operations may play a role at this altitude level. Particularly at high altitudes, the combustion efficiency of aircraft engines may be reduced due to the thinning of the atmosphere, leading to changes

in emission components. Furthermore, acoustic propagation may be more affected by changes in air temperature and pressure. In addition, the correlation coefficients between  $\text{SO}_2$  and  $L_{den}$  showed relatively low levels at all altitude levels (0.52 at low altitude, 0.47 at medium altitude, and 0.63 at high altitude), which may indicate that the emissions of  $\text{SO}_2$  do not correlate as closely with the noise level as  $\text{NO}_x$ . The correlation analysis in this study reveals the pattern of correlation between pollutants and noise levels in airport environments at different altitudes.

### 3.5. Emissions of gaseous pollutants from the main models of the LTO cycle per unit at airports of different altitudes

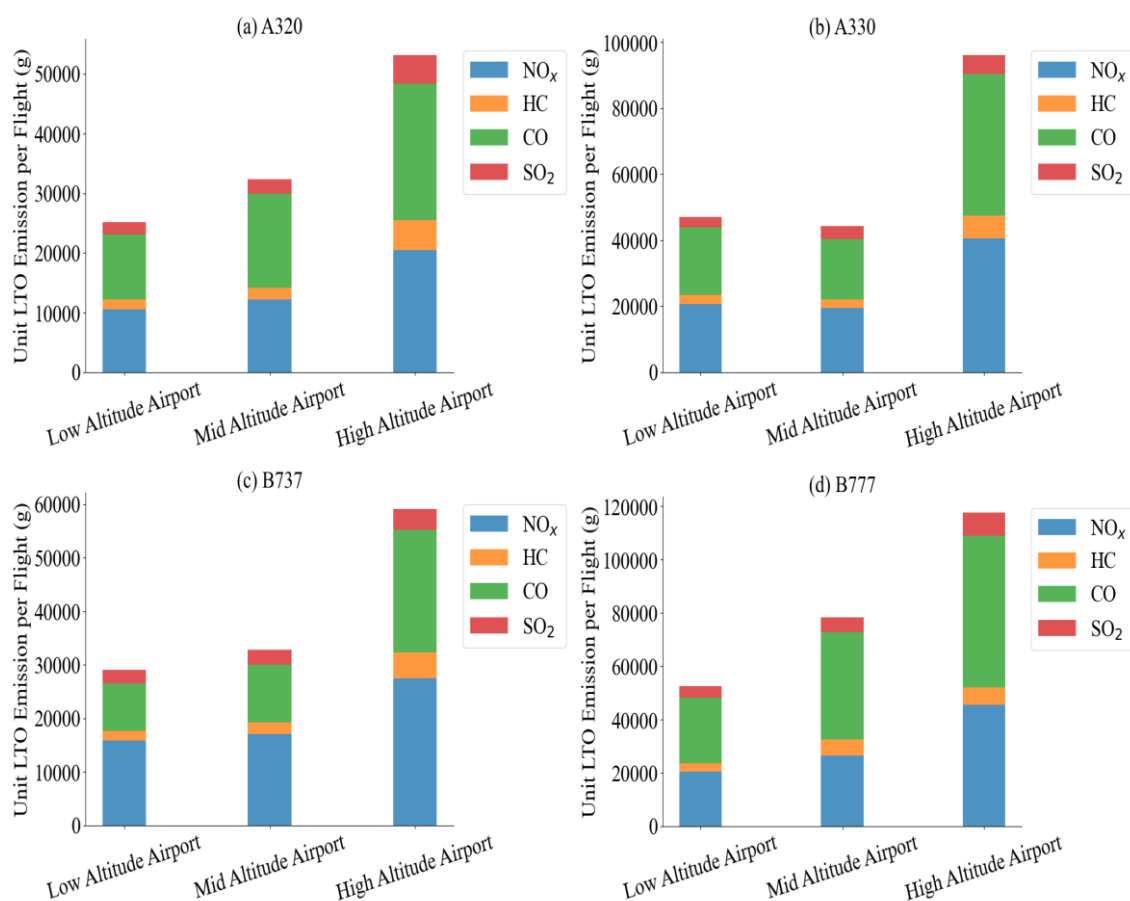


**Figure 7.** Emissions per unit LTO cycle at airports of different altitudes for aircraft types: (a) A320, (b) A330, (c) B737, and (d) B777.

The top 4 civil aviation aircraft types with different altitude airports' share were selected for comparison, and Figure 7 shows the pollutant emissions of the major aircraft types in different altitude airports' units of the LTO cycle. After comparison, the results of this study are consistent with the emission factors of the four pollutants  $\text{NO}_x$ , HC, CO, and  $\text{SO}_2$  specified by ICAO. As shown in the figure, among the four models, the emissions of  $\text{SO}_2$  and HC are significantly different compared to the other two emissions ( $\text{NO}_x$  and CO) in the unit LTO cycle regardless of the altitude airport. For airports at different altitudes, the emissions of  $\text{SO}_2$  and HC increase significantly with increasing altitude, especially from medium to high altitude, for the A320 model,  $\text{NO}_x$  and CO increase by 67.8% and 45.5%, respectively, while  $\text{SO}_2$  and HC increase by as much as 95.6% and 152.7%. This is probably due to the fact that with increasing altitude, the combustion efficiency of the aircraft engines decreases

due to the thinning of the atmosphere, which results in an increase in emissions. However, for low to medium altitude airports, the increase in the amount of emissions with the increase in altitude is not very significant, for example, in the A320 model  $\text{NO}_x$ , HC, CO, and  $\text{SO}_2$  increased only by 3.2%, 4.3%, 10.5%, and 8.5% respectively. Across different models, the total amount of cyclic emissions per unit of LTO at low altitude airports is the smallest for the A320, followed by the B737, followed by the A330, and the largest for the B777, which amounts to around 50000 g, which is nearly twice as much as that of the A320 model.

At medium altitude airports, the order of total emissions from smallest to largest is B737, A320, A330, B777, with the total amount of B777 reaching 80000 g, which is about 2.4 times as much as that of the A320 model, 2.5 times as much as that of the B737 model, and 2 times as much as that of the A330 model; under the conditions of high-altitude airports, the order of the total amount of The order from smallest to largest is A320, B737, A330, B777, and it can be seen from the graph that for most of the models, the total emissions are lower for low altitude airports than for medium altitude airports and lower for high altitude airports under different altitude conditions. However, for the A330 model, the total emissions at medium altitude airports are slightly lower than at low altitude airports. For the four types of airplanes, it can be clearly seen that the total amount of emissions at high altitude airports is much higher than that at low and medium altitude airports, in which the emissions of the A320 model at high altitude airports are the lowest at 53,184.5 g, and the B777 model is the highest, at 117,747.9 g, which is about 2.2 times as much as the total amount of the A320. The figure shows that the B777 model is the model with the highest total pollutant emissions per unit LTO cycle compared to other models, regardless of the type of airport at altitude.

#### 4. Conclusions

In this paper, an airport environmental impact assessment of the air pollutant and noise emission inventories of airports at different altitudes was carried out based on the LTO cycle, and the results showed that.

- 1) The impact of airport altitude on aircraft emissions of atmospheric pollutants and noise levels varies significantly. As the altitude increases, the emissions of  $\text{NO}_x$  and CO exhibit an upward trend, whereas the  $L_{den}$  values show a decreasing trend. The variation in altitude has a relatively minor effect on the emissions of  $\text{SO}_2$  and HC.
- 2) Notable discrepancies in emission patterns were detected among aircraft operating at different altitude airports across the LTO cycle stages. At low-altitude sites, the  $\text{NO}_x$  emissions during the climb phase constituted 45.6% of the total output, while at high-altitude airports, this figure surged to 71.8%. Furthermore, for HC and CO, high-altitude airports displayed higher shares in the taxiing phase—95.4% for HC and 97.1% for CO—contrasting with low-altitude airports' respective percentages of 84.4% and 86.1%. These trends reflect adjustments in engine operational efficiency under diverse altitude circumstances.
- 3) The emission levels of key gaseous pollutants per LTO cycle for principal aircraft models show an increasing trend with altitude. The A320 model exhibited a rise in  $\text{NO}_x$  emissions from 10.55 kg/cycle at low altitude to 20.48 kg/cycle at high altitude, with CO emissions escalating from 10.88 kg/cycle to 22.89 kg/cycle. Among the various aircraft types studied, the B777 emerged as the highest emitter across all altitude airports, as it increased fuel consumption at high altitudes to maintain consistent thrust contributed to a marked escalation in pollution outputs.
- 4) A robust correlation was established between  $\text{NO}_x$  emissions and  $L_{den}$  at airports of differing altitudes. At low-altitude locations, the correlation coefficient between  $\text{NO}_x$  emissions

and  $L_{den}$  reaches 0.96, indicating that increased air traffic density and warmer environmental conditions significantly enhance  $\text{NO}_x$  production, thereby influencing noise levels. Similar strong correlations were observed at medium-altitude (0.97) and high-altitude (0.93) airports, which may reflect the impact of atmospheric pressure and temperature variations on engine combustion efficiency, thus indirectly affecting noise levels.

### Use of AI tools declaration

The authors declare they have not used Artificial Intelligence (AI) tools in the creation of this article.

### Author contributions

Conceptualization, methodology, WZ.Tang.; software, J.Dai.; validation, ZS.Huang.; investigation, J.Dai. and ZS.Huang.; resources, WZ.Tang.; data curation, J.Dai.; writing—original draft preparation, J.Dai.; writing—review and editing, WZ.Tang. and J.Dai.; visualization, ZS.Huang.; supervision, WZ.Tang.; project administration, WZ.Tang.; funding acquisition, WZ.T. All authors have read and agreed to the published version of the manuscript.

### Conflict of Interest

The authors declare no conflict of interest.

### References

1. Dessens O, Kohler M O, Rogers H L, et al. (2014) Aviation and climate change. *Transport Policy* 34: 14–20. <https://doi.org/10.1016/j.tranpol.2014.02.014>
2. Chu YP (2013) Impacts of aircraft exhaust emissions on air quality in the vicinity of Shanghai Pudong International Airport. *Environ Monit Early Warning* 5: 50–52+56. <https://doi.org/10.3969/j.issn.1674-6732.2013.04.016>
3. Stettler ME, Eastham S, Barrett SRH (2011) Air quality and public health impacts of UK airports. part I: Emissions. *Atmos Environ* 45: 5415–5424. <https://doi.org/10.1016/j.atmosenv.2011.07.012>
4. Wilcox LJ, Shine KP, Hoskins BJ (2012) Radiative forcing due to aviation water vapour emissions. *Atmos Environ* 63: 1–13. <https://doi.org/10.1016/j.atmosenv.2012.08.072>
5. Meister J, Schalcher S, Wunderli JM, et al. (2021) Comparison of the aircraft noise calculation programs sonAIR, FLULA2 and AEDT with noise measurements of single flights. *Aerospace* 8: 388. <https://doi.org/10.3390/aerospace8120388>
6. Ollerhead J, Sharp B (2001) MAGENTA-Assessments of Future Aircraft Noise Policy Options. *Air Space Europe* 3: 247–249. [https://doi.org/10.1016/S1290-0958\(01\)90108-X](https://doi.org/10.1016/S1290-0958(01)90108-X)
7. Mato RR, Mufuruki TS (1999) Noise Pollution Associated with the Operation of the Dar Es Salaam International Airport. *Transport Res D-Tr E* 4: 81–89. [https://doi.org/10.1016/S1361-9209\(98\)00024-8](https://doi.org/10.1016/S1361-9209(98)00024-8)
8. Xia Q (2012) Aircraft Engine Emission Impact Assessment of Airports on the Atmospheric Environment. *Nanjing U Aeronaut Astronaut*. <https://doi.org/10.7666/d.y1855019>

9. Hudda N, Fruin SA (2015) International airport impacts to air quality: size and related properties of large increases in ultrafine particle number concentrations. *Environ Sci Technol* 50: 3362–3370. <https://doi.org/10.1021/acs.est.5b05313>
10. Kampa M, Castanas E (2008) Human health effects of air pollution. *Environ Pollut* 151: 362–367.
11. Wasiuk DK, Khan MAH, Shallcross DE, et al. (2016) A commercial aircraft fuel burn and emissions inventory for 2005–2011. *Atmosphere* 7: 78. <https://doi.org/10.3390/atmos7060078>
12. Cao HL, Miao JH, Miao LY, et al. (2019) Study on the estimation method of daily emission inventory of aircraft engines at the capital airport based on actual flight data. *J Environ Sci* 39: 2699–2707. <https://doi.org/10.13671/j.hjkxxb.2019.0048>
13. Li J, Zhao ZQ, Liu XK, et al. (2018) Computational analysis of aircraft emission inventory at Capital International Airport. *China Environ Sci* 38: 4469–4475. <https://doi.org/10.3969/j.issn.1000-6923.2018.12.009>
14. Xu R, Lang JB, Yang XW, et al. (2016) Establishment of an aircraft emission inventory at the Capital International Airport. *China Environ Sci* 36: 2554–2560. <https://doi.org/10.3969/j.issn.1000-6923.2016.08.038>
15. Xu R, Lang JB, Cheng SY, et al. (2017) Inventory of mobile source air pollutant emissions at the Capital International Airport. *J Safety Environ* 17: 1957–1962. <https://doi.org/10.13637/j.issn.1009-6094.2017.05.065>
16. Wang YN, Sun NX, Feng JH, et al. (2023) Emissions from Beijing Daxing International Airport and their environmental impacts and predictions. *J Environ Sci* 43: 153–165. <https://doi.org/10.13671/j.hjkxxb.2022.0426>
17. Li N, Sun Y, Gao Z (2019) Computational analysis of aircraft emission inventory at Pudong International Airport. *Aviat Comput Technol* 49: 15–19. <https://doi.org/10.3969/j.issn.1671-654X.2019.03.004>
18. Huang QF, Chen GN, Hu DX, et al. (2014) Analysis of air pollutant emissions from aircraft at Guangzhou Baiyun International Airport. *Environ Monit Manage Technol* 26: 57–59. <https://doi.org/10.3969/j.issn.1006-2009.2014.03.022>
19. Wang RL, Cheng H, Ren HJ, et al. (2018) Inventory of air pollutant emissions from the takeoff and landing (LTO) cycle of civil aircraft in the Yangtze River Delta region. *J Environ Sci* 38: 4472–4479. <https://doi.org/10.13671/j.hjkxxb.2018.0262>
20. Han B, Kong WK, Yao TW, et al. (2020) Inventory of air pollutant emissions from aircraft LTO in the Beijing-Tianjin-Hebei airport cluster. *Environ Sci* 41: 1143–1150. <https://doi.org/10.13227/j.hjcx.201908199>
21. Du YY (2022) Prediction and prevention of aircraft noise pollution at Tianjin airport based on INM model. *Noise Vib Control* 42: 186–190. <https://doi.org/10.3969/j.issn.1006-1355.2022.02.031>
22. Cheng DL, Yi CJ, Liang ZF (2005) Research on aircraft noise and countermeasures. *Noise Vib Control* 25: 47–51. <https://doi.org/10.3969/j.issn.1006-1355.2005.05.016>
23. Mato RR, Mufuruki TS (1999) Noise Pollution Associated with the Operation of the Dar Es Salaam International Airport. *Transport Environ* 4: 277–289. [https://doi.org/10.1016/S1361-9209\(98\)00024-8](https://doi.org/10.1016/S1361-9209(98)00024-8)
24. International Civil Aviation Organization. 2014. ICAO Environmental Report 2013. International Civil Aviation Organization.



25. Wei C, Diao HZ, Han B (2014) Calculation of pollutant emissions from civil aircraft during cruise phase. *Science. Technol Eng* 14: 122–127. <https://doi.org/10.3969/j.issn.1671-1815.2014.19.023>
26. The Environment Branch of the International Civil Aviation Organization (ICAO). (2014). ICAO Environmental Report 2013. International Civil Aviation Organization.
27. Chandrasekaran N, Guha A (2012) Study of prediction methods for NO<sub>x</sub> emission from turbofan engines. *J Propuls Power* 28: 170–180. <https://doi.org/10.2514/1.B34245>
28. Huang MY, Hu R, Zhang JF, et al. (2020) Calculation and analysis of aircraft exhaust emissions based on fast access logger data. *Science. Technol Eng* 20: 13502–13507. <https://doi.org/10.3969/j.issn.1671-1815.2020.32.060>
29. Kalivoda MT, Monika K (1998) Methodologies for estimating emissions from air traffic: future emissions [R]. MEET Project ST-96-SC, 204, Vienna, Austria: Perchtoldsdorf-Vienna, 46–53.
30. ISO 20906. 2009. Acoustics-unattended monitoring of aircraft sound in the vicinity of airports.
31. Directive EU (2002) Directive 2002/49/EC of the European parliament and the Council of 25 June 2002 relating to the assessment and management of environmental noise. *Off J Eur Commun L* 189: 2002.
32. Federal Aviation Administration (1983) Noise control and compatibility planning for airports. *Advisory circular AC150-5020-1*.
33. Cao XY, Liu Q, Liu Z, et al. (2022) Assessment of pollutant emissions from the LTO cycle of Chinese civil aviation aircraft. *Environ Sci Technol* 45: 116–124. <https://link.cnki.net/doi/10.19672/j.cnki.1003-6504.2303.21.338>
34. Wu ZB (2017) Research on fuel ignition characteristics and combustion enhancement in high altitude environment. University of Science and Technology of China.
35. Dai SP, Jia XH, Ding SJ, et al. (2024) Experimental study on the combustion characteristics of small-scale oil pool fire in restricted space in plateau. *Fire Sci Technol* 43: 161–167. <https://doi.org/10.3969/j.issn.1009-0029.2024.02.004>
36. Liu QY, Zhu WT, Zhu B, et al. (2021) Study on combustion characteristics of combustible liquids under high plateau airport environment. *Fire Sci Technol* 40: 613–616. <https://doi.org/10.3969/j.issn.1009-0029.2021.05.003>



AIMS Press

© 2024 the Author(s), licensee AIMS Press. This is an open access article distributed under the terms of the Creative Commons Attribution License (<https://creativecommons.org/licenses/by/4.0>)